

ADVANCED MATERIALS

Supporting Information

for *Adv. Mater.*, DOI: 10.1002/adma.202007900

Metal-Bridged Graphene–Protein Supraparticles for
Analog and Digital Nitric Oxide Sensing

*Zhi-Bei Qu, Xinguang Zhou, Min Zhang, Jianlei Shen,
Qian Li, Feng Xu,* Nicholas Kotov,* and Chunhai Fan**

Copyright 2021 Wiley-VCH GmbH

Supporting Information

Metal-Bridged Graphene-Protein Supraparticles for Analog and Digital Nitric Oxide Sensing

Zhibei Qu^{1,2}, Xinguang Zhou^{3,4}, Min Zhang⁴, Jianlei Shen², Qian Li², Feng Xu^{1*}, Nicholas Kotov^{5*}, Chunhai Fan^{2,6*}

¹Joint Research Center for Precision Medicine, Shanghai Jiao Tong University & Affiliated Sixth People's Hospital South Campus, Southern Medical University Affiliated Fengxian Hospital, Shanghai 201400, China.

²School of Chemistry and Chemical Engineering, Frontiers Science Centre for Transformative Molecules, Shanghai Jiao Tong University, Shanghai 200240, China.

³Shenzhen NTEK Testing Technology Co., Ltd., Building E in Fenda Science Park, Baoan District, Shenzhen 518000, China.

⁴School of Chemistry and Molecular Engineering, East China Normal University, Shanghai, 200241, China.

⁵Department of Chemical Engineering, Biointerfaces Institute, University of Michigan, Ann Arbor, MI 48109, USA.

⁶Institute of Molecular Medicine, Shanghai Key Laboratory for Nucleic Acids Chemistry and Nanomedicine, Renji Hospital, School of Medicine, Shanghai Jiao Tong University, Shanghai 200127, China

*E-mail: xuf@smu.edu.cn; kotov@umich.edu; fanchunhai@sjtu.edu.cn.

Experimental Section :

Chemicals. SOD protein was purchased from Sangon, Inc. (Shanghai, China). Tb(NO₃)₃ and other lanthanide nitric salts were purchased from Diyang Chemical (Shanghai) Co., Ltd. 4,5,-diaminofluorescein (DAF-2) was provided by Sigma Aldrich. All other reagents are of analytical

reagent grade, purchased from Shanghai Sinopharm. Group Co. All solutions were prepared using ultrapure water from a Milli-Q ultrapure water system.

Synthesis of graphene quantum dots (GQDs). GQDs were synthesized by a modified protocol through a top-down “oxidation-cutting” process¹. In detail, 50 mg of carbon fibres was dispersed into a 4 mL mixture of sulphuric acid and nitric acid (3:1 v/v). The black solution was sonicated for 2 h and mechanically stirred for 24 h at 80 °C. After the reaction, the mixture was cooled and diluted with deionized (DI) water (0.15 mg/mL). Sodium hydroxide was added into the solution to adjust the pH value to neutral. The mixture was further dialyzed (molecular weight: 3500 Da) for 3 days to obtain the final product.

Synthesis of SPs. The GQD nanochains were self-assembled by adding lanthanide metal ions (e.g., Tb³⁺ ions) to a dispersion of GQDs. Typically, HCl solution was added into 0.01 mg/mL GQDs to keep a weakly acidic pH of around 5-6. SOD protein solutions with different concentration were slowly mixed with GQDs under mild shaking and then the Tb³⁺ (1 mM) solution was added. The mixture was stored at room temperature overnight until the yellow-brown color of the solution turned slightly darker. The product was further purified using an ultrafiltration tube (molecular weight cutoff: 3000 Da) then placed in a centrifuge for 0.5 h (6000 rpm) three times.

Instrumentation. TEM employed in the characterization is Talos L120C G2 (FEI, USA). SEM (TESCAN, MIRA3 FE-SEM) was performed for the morphological studies of the nanoassemblies. The elemental analysis was performed by XPS (Kratos, Axis Ultra XPS). To

confirm the accuracy and reliability of the data, the XPS in this experiment was calibrated by the means of Au 4f 7/2 peak at 84.00 eV from gold film coating on a blank sample on silicon wafer.

The fluorescence emission properties of GQDs and their assemblies were investigated by fluorescence spectroscopy (Horiba, Fluoromax-3PLUS). The absorbance of the samples was analysed by UV-Vis spectroscopy (Perkin-Elmer, Lambda 850). The circular dichroism was analysed by CD spectroscopy (JASCO, J-815). Confocal fluorescence microscopy (Leica, SP8 MP) was applied in the single particle fluorescence tracking. A plate reader (Molecular Devices, SpectraMax iD5) was used for the high-throughput fluorescent detection for the quantitative experiments. The fluorescence lifetime was measured by a steady/transit fluorescence spectrometer (Edinburg, FLS1000).

DFT calculations and MD simulations. Density functional theory (DFT) calculations were performed to obtain the optimized geometrical parameters, vibrational frequencies, and orbital energies of the terbium-GQD/amino acid coordination assemblies and copper complexes. DFT calculations were performed using GAUSSIAN 09 (version: Rev. E.01, 2015) software package and GAUSSVIEW 5.0 visualization program. Water molecules completed the coordination sphere of the lanthanide ions forming seven coordination bonds around them². The copper complexes were adapted from the surrounding amino acids and corresponding copper ions in SOD protein. Tb³⁺ is described using the relativistic 4f-in-core pseudopotential (also named as large-core RECP) and a corresponding triple-zeta basis set (ECP54MWB-II) for valence electrons^{3,4}, while polarized basis sets of triple-zeta quality (def2-tzvp) were used for the H, C, N, and O atoms⁵. Copper (II) has one unpaired electron, so unrestricted functional B3LYP⁶ with

LANL2DZ basis set⁷ was used for an open-shell electronic structure, whereas singlet close-shell B3LYP/LANL2DZ setting was applied for Cu (I). The ground state was converged to the threshold of 10^{-4} Hartree/Å on the Cartesian gradients while the energy was converged to a tight threshold of 10^{-6} Hartree. Frequency analyses were used to verify that the optimized structures were at their least local minimum that no imaginary frequencies were found in the final structures. Ultrafine integration grids were employed for all the calculations. For other computational details, please refer to the output (.log) files in supplementary information.

Molecular dynamics (MD) simulations were performed with the GROMACS package version 2019 beta1⁸, with the universal force field (UFF) for all-atom simulations⁹ and Martini v2.2 force field parameters for coarse-grained simulations¹⁰. For the UFF settings, OBGMX was applied to generate the topological files¹¹. The SOD structure was imported from RCSB Protein Data Bank (PDB) website (pdb ID: 2z7u). The structure was further coarse-grained (CG) to reduce the computational cost, in a solvation box using polarized CG water molecules (**Figure S8**). The hydrated Tb³⁺ ion forcefield was adapted from a previous report¹². The molecular ratio of Tb³⁺ to SOD protein was set to 1000:1. The extra charges were balanced with Cl⁻ ions. After initial energy minimization with position restraints applied on the protein beads, short equilibrium processes were performed with the position restraints applied to the protein backbone beads. All simulations were performed with a time step of 10 fs and a set temperature of 300 K, with velocity-rescaling thermostats,¹³ with a time constant for coupling of 1 ps. An isotropic pressure of 1 bar was maintained with the Berendsen barostat¹⁴, with a compressibility of 3×10^{-4} bar⁻¹, and a relaxation time constant of 5 ps. Production runs with a duration of 10 μs were used to obtain the final data.

Breath collection and NO detection from human subjects. The human subjects exhaled gas were obtained under the Institutional Review Board (IRB) approval of Shanghai Jiao Tong University (SJTU). All participants involved in the study understood the information of the project and formally confirmed. A detailed report, consisting of experimental protocols and data processing, was submitted to the Ethics Committee of SJTU. The exhaled breath samples of the volunteers ($n = 3$) were collected by homemade breath samplers, adapted from a previously reported protocol¹⁵, using a 50 mL plastic injector refitted breath sampler. To avoid any possible contamination from oral infection or dental plague, volunteers were requested to carefully wash their mouths using *Listerine* mouthwash. After that, the volunteers were asked to inhale and exhale air in a normal fashion four times. After four normal breaths, referring to the “resting breathing” method, the subject inhaled to the full capacity of the lungs and then exhaled for ~ 30 s, with a flow in the range of 10-50 mL/s. Three breath measurements were taken for each individual. The collected breath samples were then slowly injected into the bottom of a vial containing 10 mL SPs solution in 10 mM HEPES buffer solution, where the injection was controlled at a flow rate of 5 mL/min using a flowmeter. Then 1 mL of the SPs solution was used for fluorescence measurements. To enhance the signal-noise ratio, time-resolved fluorescence (TRF)¹⁶ of terbium was employed. The fluorescence at 545 nm was collected for quantitation of NO concentrations, using 290 nm excitation with a delay-time of 100 μ s. For the standard reference of NO quantitation, 10 μ M DAF-2 solution in 10 mM PBS (pH 7.4) was applied. The fluorescence at 515 nm was collected using 490 nm excitation. The LOD was computed by fitting the fluorescence intensity, as a function of concentration of NO to a linear regression. The

LOD was defined as the intersection of the lower 95% confidence bound of the fit with the upper 95% confidence bound of the blank measurements.

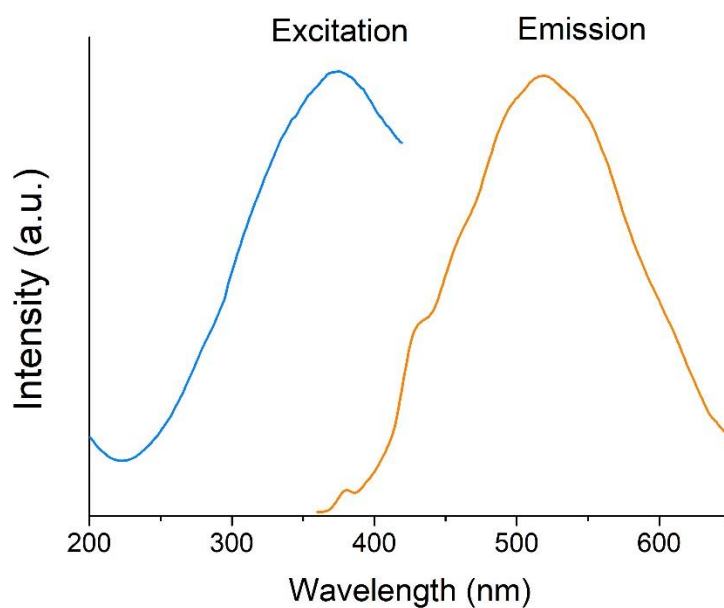


Figure S1. Excitation and emission spectra for the fluorescence of GQDs. The excitation spectrum was collected at 520 nm fluorescence, while the emission spectrum was collected using 365 nm excitation.

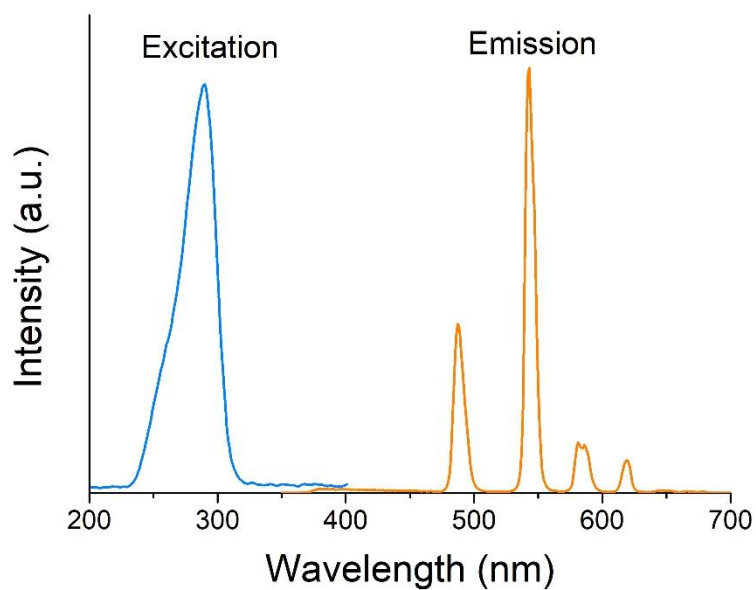


Figure S2. Excitation and emission spectra for the fluorescence of SPs. The excitation spectrum was collected at 545 nm fluorescence, while the emission spectrum was collected using 290 nm excitation.

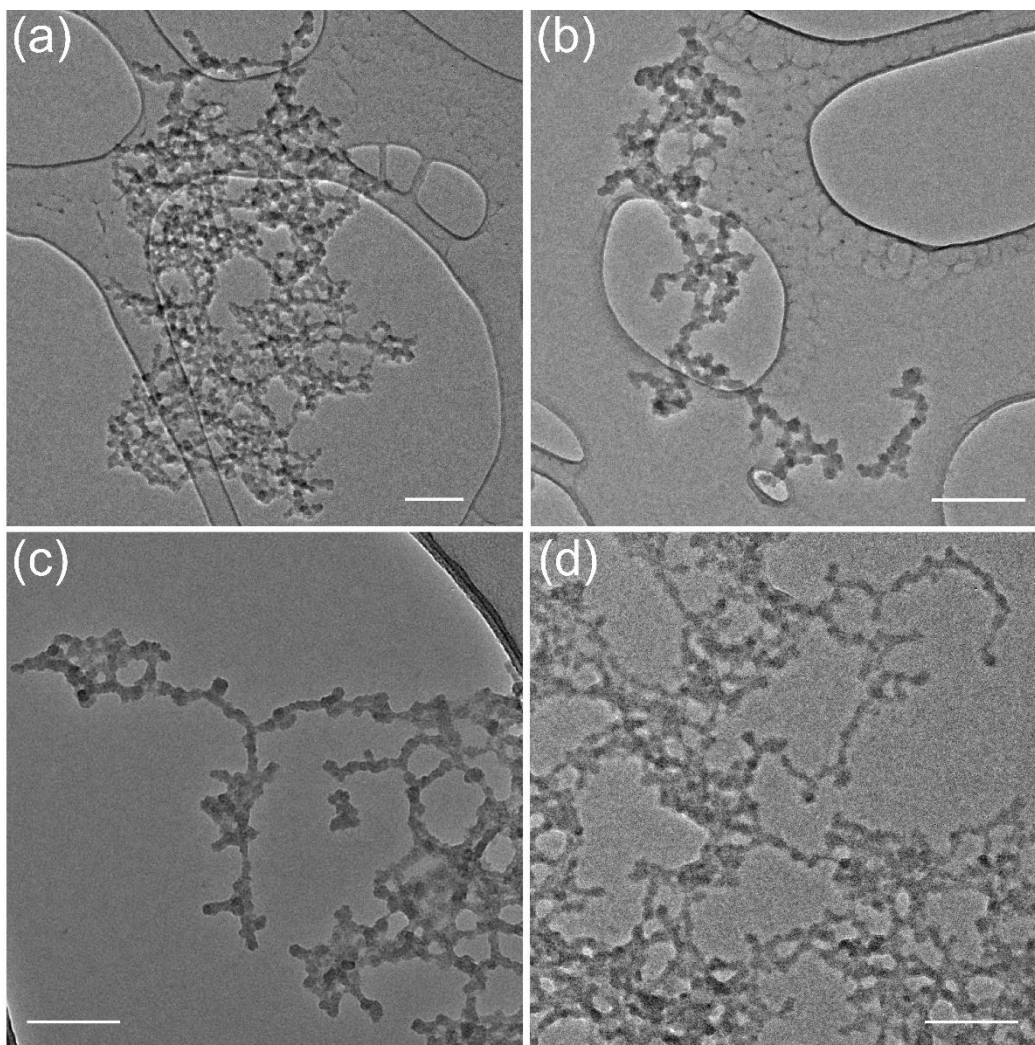


Figure S3. TEM images of GQD assemblies induced by lanthanide ions (a) Y^{3+} , (b) Eu^{3+} , (c) Ce^{3+} , and (d) Gd^{3+} . $[\text{GQD}] = 0.1 \text{ mg/mL}$, $[\text{Ln}^{3+}] = 1 \text{ mM}$. Scale bar: 200 nm.

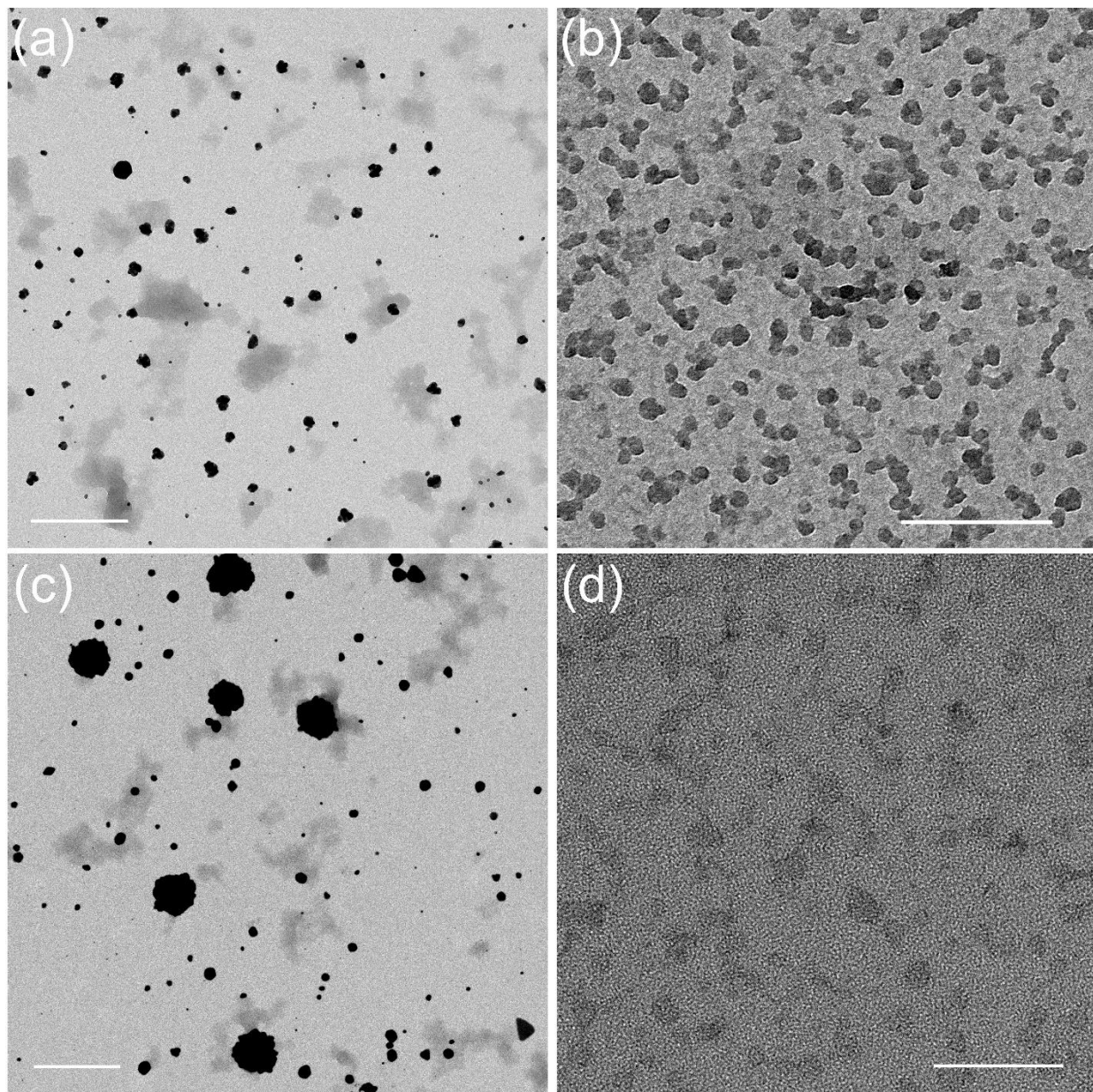


Figure S4. TEM images of GQD-Ln³⁺-SOD SPs induced by lanthanide ions (a) Y³⁺, (b) Eu³⁺, (c) Ce³⁺, and (d) Gd³⁺. [GQD] = 0.1 mg/mL, [SOD] = 0.8 mg/mL, [Ln³⁺] = 1 mM. Scale bar: 200 nm.

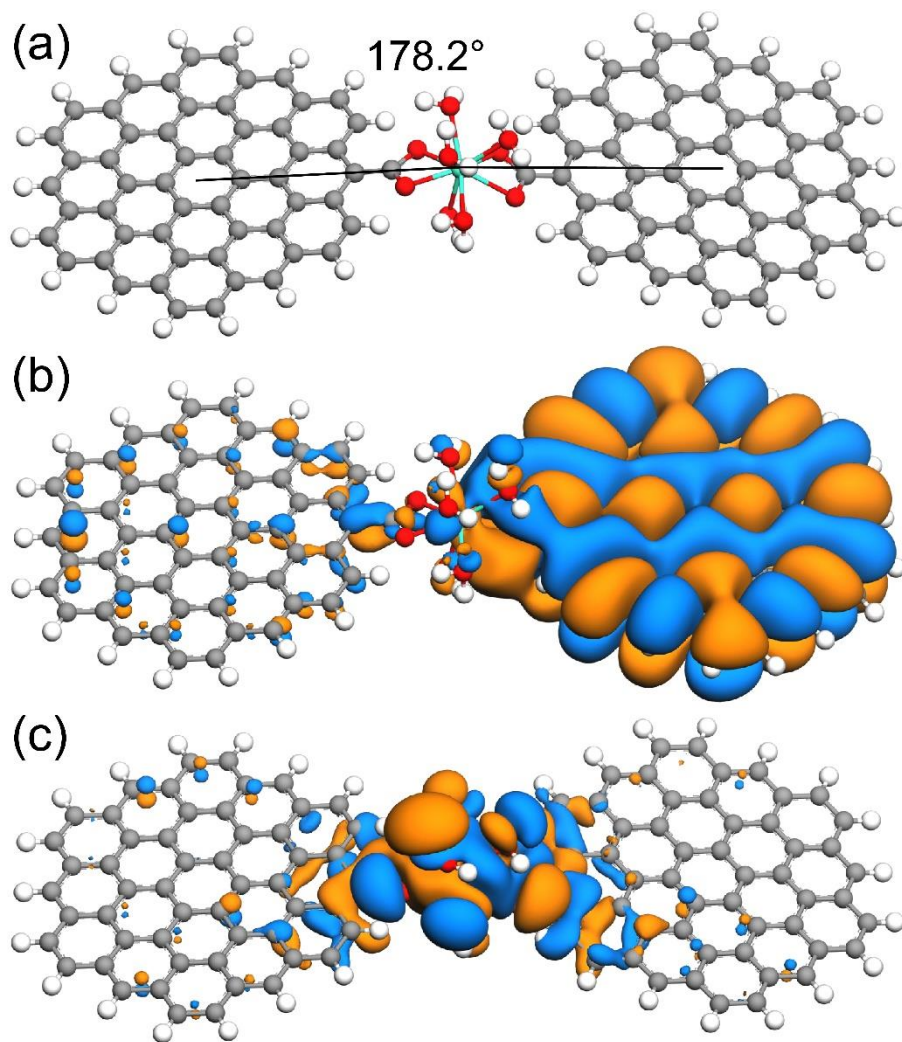


Figure S5. Optimized geometry of (a), LUMO (b) and HOMO (c) for GQD-Tb³⁺-GQD coordination assembly from DFT calculations.

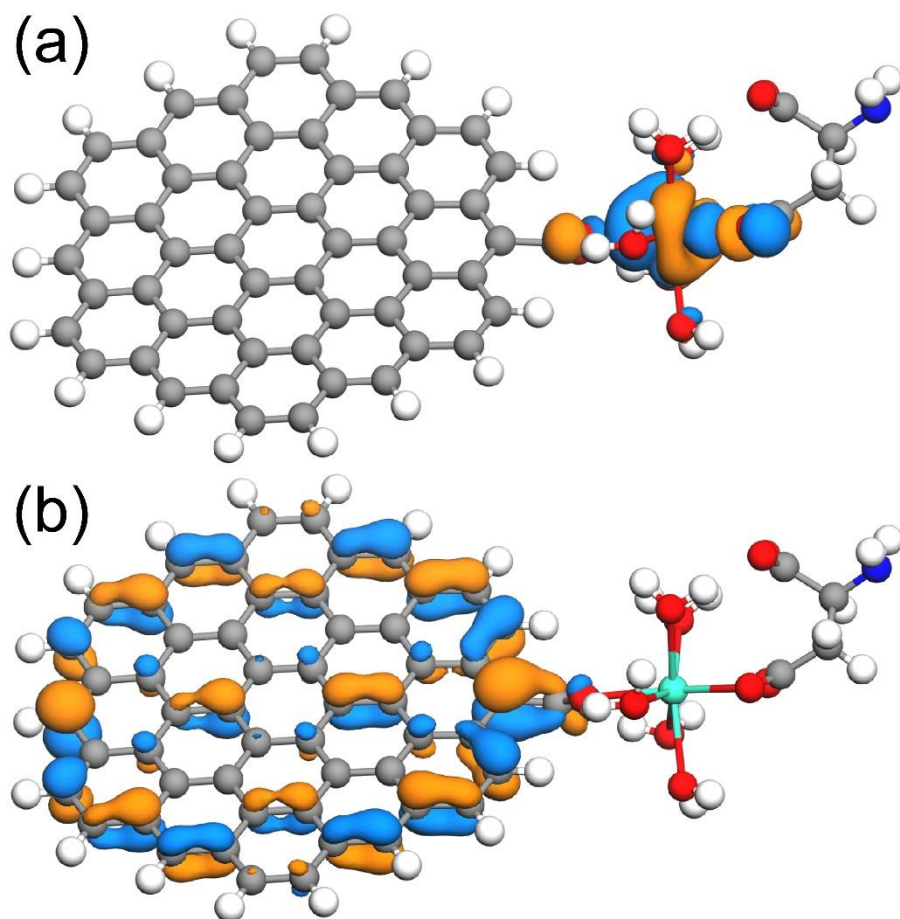


Figure S6. Plotted molecular orbitals isosurfaces for LUMO (a) and HOMO (b) for GQD-Tb³⁺-Asp coordination assembly from DFT calculations.

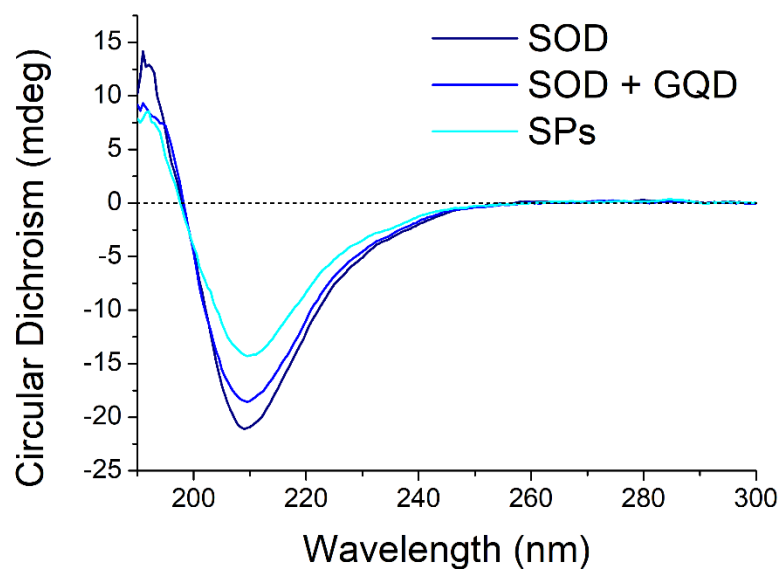


Figure S7. Circular dichroism (CD) spectra for SOD (dark blue), mixture of SOD and GQD (blue), and the SPs (light blue). The concentration of SOD was 0.1 mg/mL in all cases.

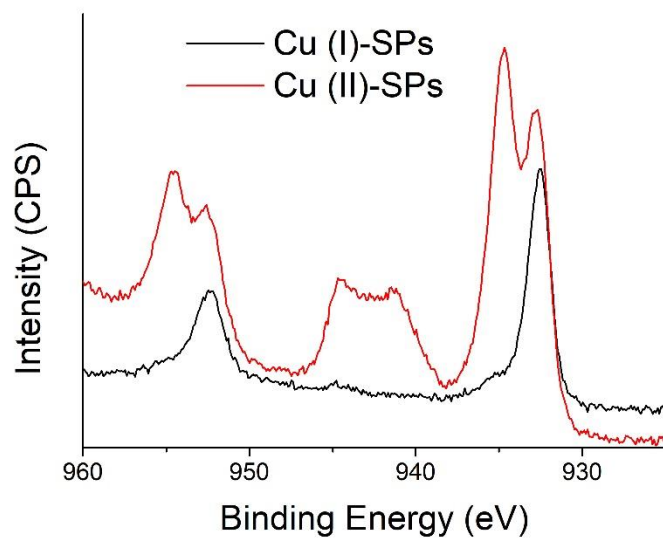


Figure S8. High resolution XPS spectra of copper 2p_{2/3} for Cu (I)-SPs (black) and Cu (II)-SPs (red).

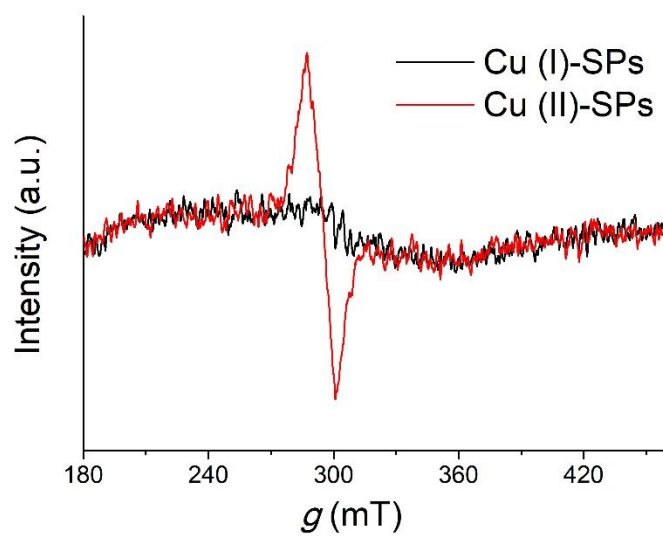


Figure S9. EPR spectra at 107 K for Cu (I)-SPs (black) and Cu (II)-SPs (red).

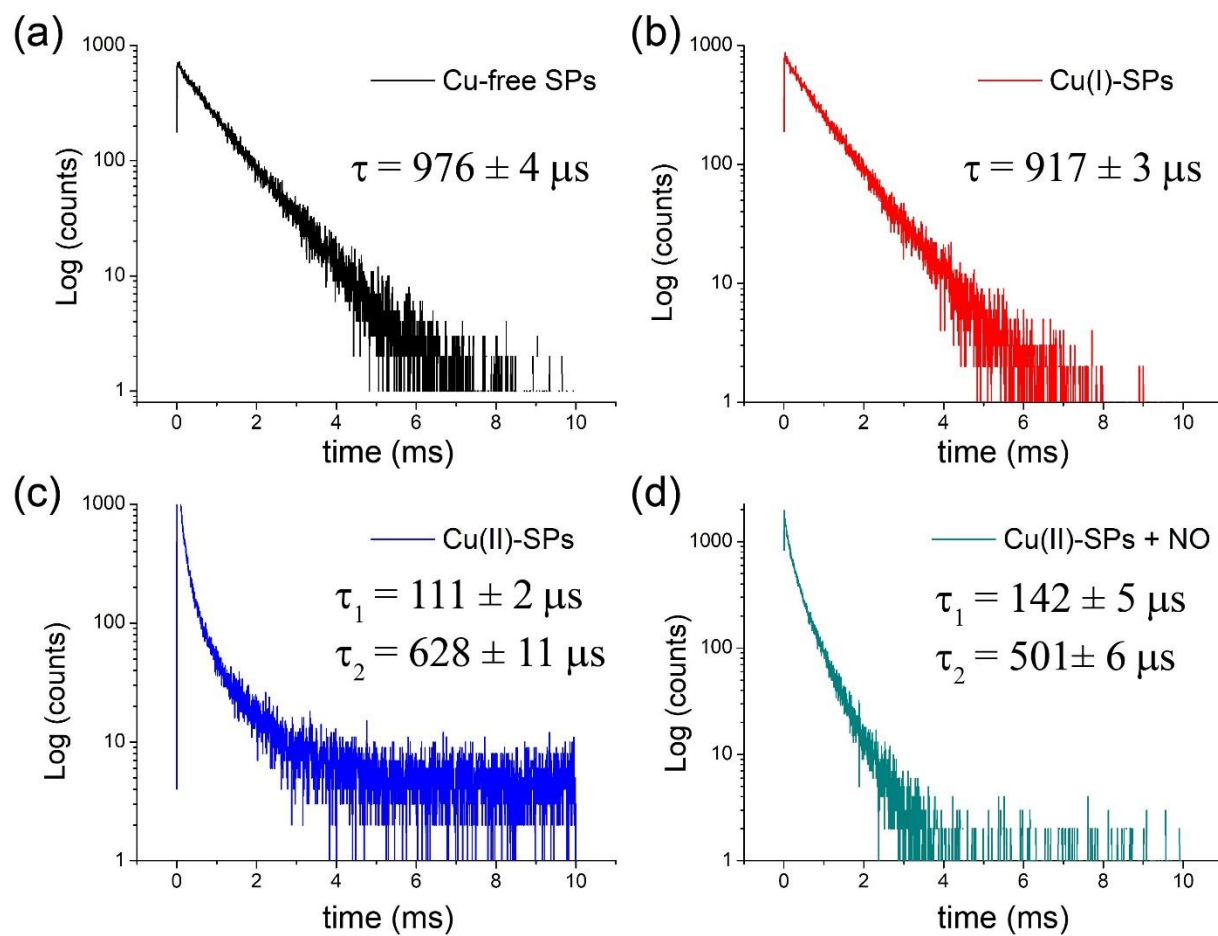


Figure S10. Fluorescence lifetime plots and corresponding lifetimes for the SPs of (a) copper-free, (b) Cu (I), (c) Cu (II) and (d) Cu (II) in the presence of NO.

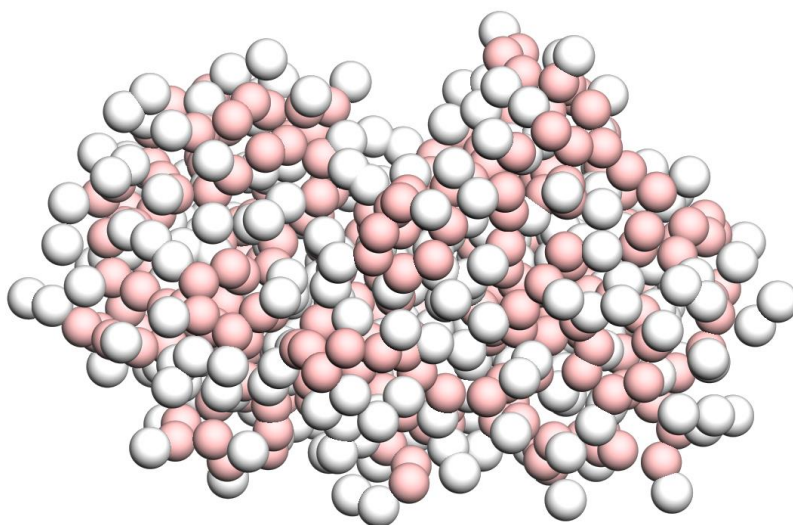


Figure S11. Snapshot of SOD from coarse-grained MD simulations using Martini method¹². Pink ball: backbone bead, white ball: sidechain bead of protein residues.

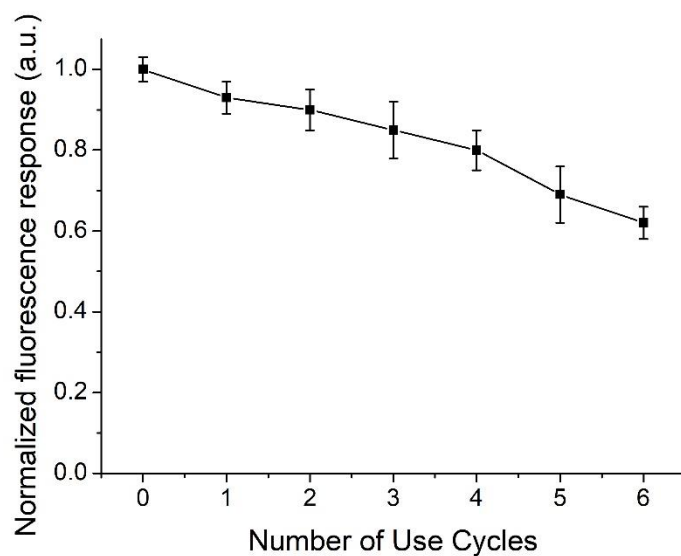


Figure S12. Reusability of the SP-based NO sensors. Normalized fluorescence responses of recovered SPs to NO after a number of cycles of centrifugation and reactivation by H_2O_2 . The reduction of normalized fluorescence response is likely to be related to partial disassembly of SPs during redispersion to attain the quasi-equilibrium state.

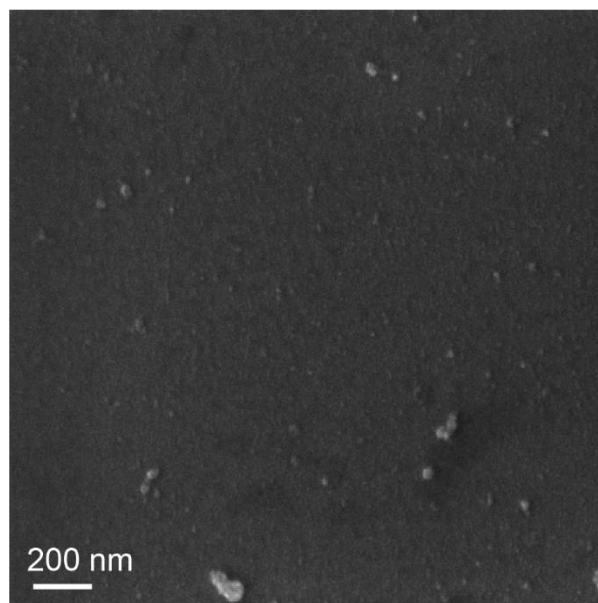


Figure S13. SEM image for the SPs used in the calculations of the particle density in single particle fluorescence experiments.

References

1. Peng, J. *et al.* Graphene quantum dots derived from carbon fibers. *Nano Lett.* **12**, 844–849 (2012).
2. Bünzli, J.-C. G. & Vuckovic, M. M. Spectroscopic properties of anhydrous and aqueous solutions of terbium perchlorate and nitrate: Coordination numbers of the Tb(III) ion. *Inorganica Chim. Acta* **73**, 53–61 (1983).
3. Guillaumont, D., Bazin, H., Benech, J.-M., Boyer, M. & Mathis, G. Luminescent Eu(III) and Gd(III) Trisbipyridine Cryptates: Experimental and Theoretical Study of the Substituent Effects. *ChemPhysChem* **8**, 480–488 (2007).
4. Yang, J. & Dolg, M. Valence basis sets for lanthanide 4f-in-core pseudopotentials adapted for crystal orbital ab initio calculations. *Theor. Chem. Acc.* **113**, 212–224 (2005).
5. Weigend, F. & Ahlrichs, R. Balanced basis sets of split valence, triple zeta valence and quadruple zeta valence quality for H to Rn: Design and assessment of accuracy. *Phys. Chem. Chem. Phys.* **7**, 3297–3305 (2005).
6. Barone, V. & Cossi, M. Quantum Calculation of Molecular Energies and Energy Gradients in Solution by a Conductor Solvent Model. *J. Phys. Chem. A* **102**, 1995–2001 (1998).
7. Check, C. E. *et al.* Addition of Polarization and Diffuse Functions to the LANL2DZ Basis Set for P-Block Elements. *J. Phys. Chem. A* **105**, 8111–8116 (2001).
8. Van Der Spoel, D. *et al.* GROMACS: Fast, flexible, and free. *J. Comput. Chem.* **26**, 1701–1718 (2005).
9. Rappe, A. K., Casewit, C. J., Colwell, K. S., Goddard, W. A. & Skiff, W. M. UFF, a full periodic table force field for molecular mechanics and molecular dynamics simulations. *J. Am. Chem. Soc.* **114**, 10024–10035 (1992).
10. Monticelli, L. *et al.* The MARTINI Coarse-Grained Force Field: Extension to Proteins. *J. Chem. Theory Comput.* **4**, 819–834 (2008).
11. Garberoglio, G. OBGMX: A web-based generator of GROMACS topologies for molecular and periodic systems using the universal force field. *J. Comput. Chem.* **33**, 2204–2208 (2012).
12. Michalowsky, J., Zeman, J., Holm, C. & Smiattek, J. A polarizable MARTINI model for monovalent ions in aqueous solution. *J. Chem. Phys.* **149**, 163319 (2018).
13. Bussi, G., Donadio, D. & Parrinello, M. Canonical sampling through velocity rescaling. *J. Chem. Phys.* **126**, 14101 (2007).
14. Berendsen, H. J. C., Postma, J. P. M., van Gunsteren, W. F., DiNola, A. & Haak, J. R. Molecular dynamics with coupling to an external bath. *J. Chem. Phys.* **81**, 3684–3690 (1984).
15. Robinson, J. K., Bollinger, M. J. & Birks, J. W. Luminol/H₂O₂ Chemiluminescence Detector for the Analysis of Nitric Oxide in Exhaled Breath. *Anal. Chem.* **71**, 5131–5136 (1999).
16. Xue, S. F. *et al.* DNA Encountering Terbium(III): A Smart ‘chemical Nose/Tongue’ for Large-Scale Time-Gated Luminescent and Lifetime-Based Sensing. *Anal. Chem.* (2018). doi:10.1021/acs.analchem.7b05167